On the microstructural refinement in commercial purity Al and Al-10wt.% Cu alloy under ultrasonication during solidification

H.R. Kotadia[1], M. Qian[2], D.G. Eskin[3,4] and A. Das[5*]

[1] Warwick Manufacturing Group, Warwick University, Coventry CV4 7AL, UK

[2] School of Engineering, RMIT University, Melbourne, VIC 3000, Australia

[3] Brunel Centre for Advanced Solidification Technology, Brunel University London, Uxbridge UB3 PH, UK

[4]Tomsk State University, Tomsk 634050, Russia

[5] College of Engineering, Swansea University Bay Campus, Swansea, SA1 8EN, UK

Abstract:

Physical grain refinement is examined under high-intensity ultrasonication during solidification in commercial purity Al (CP-Al) and binary Al-10wt.% Cu alloy melts cooled naturally in air and compared against chemical inoculation using Al-5Ti-1B grain refiner. The coarse dendritic unrefined base microstructure was completely replaced with a fine equiaxed grain structure in the case of either inoculation or ultrasonication. However, ultrasonication produced more effective refinement over chemical inoculation with a two-fold and eight-fold increase in the grain density in CP-Al and Al-10%Cu alloy, respectively. While combining chemical inoculation with ultrasonication produced the finest grain structure in CP-Al, no further improvement over ultrasonication was noted for the Al-10%Cu alloy. Noticeable reduction in nucleation undercooling, of similar magnitude to chemical inoculation, was observed under ultrasonication. Cooling curve observations indicate strongly enhanced heterogeneous nucleation under ultrasonication. It appears that although nucleation potency could be higher under chemical inoculation, more nucleation events are favoured under cavitation.

Keywords: Grain refining; Ultrasound; Cavitation; Al-Ti-B refiner; Aluminium alloys; Solidification microstructure

* Corresponding author. Tel.: +44 1792 602031 E-mail address: a.das@swansea.ac.uk (A. Das)

1. Introduction

Chemical grain refinement is widely practiced for Al [1, 2] and Mg [3] castings in order to promote equiaxed grain formation and refine ingot or billet grain structures. Motivation for such refinement is to reduce hot tearing, improve feeding, minimise porosity and segregation, and enhance microstructural homogeneity, as well as to improve mechanical properties of as-cast components [4, 5]. The effectiveness of a specific grain refiner, however, is often dependent on alloy composition. Some of the industrially important alloys respond poorly to established refiners. For example, Zr is the preferred grain refiner for Mg-alloys but is largely ineffective in Al-containing Mg-alloys [3]. Similarly, the most popular inoculant for Al-alloys, Al-5Ti-1B master alloy, is least effective for Al-alloys containing high amounts of Si [5, 6]. Even for successful chemical inoculation, the grain refining efficiency is known to deteriorate with melt holding prior to casting (known as the 'fading effect') [7] and drastic reduction in refining performance (known as the 'poisoning effect') is observed from certain alloying elements [8]. In addition, potent nucleating particles can be susceptible to agglomeration [9] and their accumulation in finished castings can pose limitations for critical applications where the inclusion content needs to be kept to a minimum.

An emerging alternative to addressing the inherent limitations of chemical inoculation (as mentioned above) is to apply a physical field such as high-intensity mechanical shear [10], electromagnetic field [11], electric current pulse [12], or low frequency mechanical vibration [13]. Among the various physical refinement techniques, application of high-intensity ultrasound during solidification has shown promising grain refinement results for Mg-alloys [14-16], Al-alloys [14, 17-19], and TiAl alloys [20]. Direct introduction of ultrasound into the melt during solidification could be an alternative physical approach to inoculation for grain refinement in relatively low-melting alloys.

The effect of ultrasonic exposure on solidification microstructure is generally explained on the basis of non-linear phenomena caused by high-intensity sound wave propagation through the melt [14, 21]. Such phenomena are predominantly cavitation and acoustic streaming.

Above the cavitation threshold, formation, growth and collapse of tiny gas bubbles in the liquid is stated to produce shockwave pulses of 1000 atm and local microjects of 100 ms^{-1} [18]. Acoustic streaming, resulting from the attenuation of ultrasound in the melt, promotes large and small-scale steady fluid flow [21]. Although the origin of microstructural refinement is largely attributed to the cavitation phenomena, the exact mechanism(s) of such refinement is still debated. It is argued that shockwaves generated through cavitation fragment the dendrite arms, and the fluid flow resulting from acoustic streaming disperses the broken dendrite arms in the bulk melt leading to copious nucleation [17, 21-22]. Partial melting and detachment of secondary dendrite arms is also possible due to the increased fluid flow and mass transfer around the solid-liquid interface. But these mechanisms can only act when the ultrasonication is performed below the liquidus. In the case when the melt is processed above the liquidus, it is suggested that grain refinement results from enhanced nucleation on wet insoluble inclusions [18, 23]. The enhanced wetting of non-metallic particles under ultrasonication has clearly been demonstrated in oxide containing metal matrix composite [24]. Chalmers supported the idea of enhanced nucleation due to a rise in the equilibrium melting point (from Clapeyron equation) in molten alloys during the high pressure pulse generated on cavity collapse [25]. This view on ultrasonic enhanced nucleation was supported by others [15, 26].

It appears that despite the observed influence on microstructural refinement, detailed understanding of the effects of ultrasonication on microstructure formation is still lacking. Moreover, there are only a few studies on the efficiency of ultrasonic induced refinement compared to the established practice of chemical refinement under similar solidification conditions. In the present

investigation, commercial purity Al (CP-Al) as well as a model binary Al-10% Cu alloy (all compositions expressed in wt% unless otherwise stated) is used to explore and compare grain refinement under both ultrasonication and chemical inoculation, and an attempt is made to identify the origin of the microstructure refinement.

2. Experimental

CP-Al (99.5%) and binary Al-10% Cu alloy were used for the solidification experiments. The alloy was prepared by melting appropriate amounts of pure Al (99.5%) and Cu (99.9%). For each batch of experiments, around 2-3 kg of pure metal or alloy was melted and homogenised for 2 h at 725 ± 3 °C in a large clay-graphite crucible held inside an electric resistance furnace, and all experiments were performed using this melt reservoir to minimise compositional variation between individual experiments. For each experiment, melt was taken from the reservoir in clay-graphite crucibles (height 70 mm and diameter 50 mm) preheated to the melt temperature, placed on a refractory slab, and allowed to solidify under natural air cooling while undergoing ultrasonication or without processing. A schematic diagram of the experimental set up is shown in Fig. 1. The ultrasonic system consisted of an air-cooled piezoelectric 20 kHz 0.5 kW transducer and a waveguide system. A Ti-6Al-4V alloy radiator of 25 mm diameter was used to transmit the ultrasound into the melt at maximum pick-to-pick amplitude of 25 μm. For all of the ultrasonication experiments the radiator (horn) was first preheated by sonicating a batch of aluminium melt (that was discarded) to prevent any chill effect. A thermocouple was placed just below the submerged horn at the centre of the ingot, and the cooling curves were recorded using a multichannel data logging system. In the case of the alloy, the horn was introduced in the melt from the top at a melt temperature of 690 ^{o}C and withdrawn at an approximate melt temperature of 550 ^{o}C following around 420 s of application of ultrasound. For the CP-Al the

ultrasound horn was withdrawn just before the completion of solidification. No perceptible degradation or dissolution of the horn was noticed (see Table 2 for the concentration of Ti in the alloys). For experiments involving chemical grain refinement, a pre-measured quantity of an Al-5Ti-1B master alloy rod was first preheated and then added to the melt at 1% level (upper limit used in industry) to ensure adequate refinement. The melt was stirred intermittently and then taken out within 20 min (to prevent any fading effect) in a preheated clay-graphite crucible and allowed to solidify under the same cooling condition as with the ultrasonication experiments. Identical grain refiner addition level was used for solidification experiments involving simultaneous application of chemical refiner and ultrasonication. For comparison, solidification experiments were repeated from the same batch of melt under identical experimental set-up and cooling conditions but without any chemical refiner addition or introduction of ultrasonic horn in the melt. All individual experiments were conducted at least three times to ensure reproducibility.

Solidified ingots (50 mm diameter and 60 mm height) were cut along the central vertical plane, and both sections were ground and polished through standard metallographic techniques, and anodized using Barker's reagent (7 ml 48% HBF_4 in 200 ml distilled water) at 20 VDC for 70 s using a stainless steel cathode. A ZEISS Axioscop2 MAT optical microscope equipped with an automated Zeiss AxioVision image analyser was used under polarised light for microstructural investigation. Grain size was measured using a linear intercept methods and the statistical analysis of the results was performed.

3. Results

3.1 Solidification microstructure in the CP-Al ingots

Macrostructures of CP-Al ingots solidified from 725 ^{o}C under different melt treatment but identical cooling conditions are presented in Fig. 2. The base unrefined microstructure developed in

the quiescent natural cooling set-up of the present experiments consists of coarse columnar grain structure (Fig. 2a). The sample shown in Fig. 2b is chemically inoculated using Al-5Ti-1B master alloy. Substantial reduction in grain size and conversion to equiaxed grain structure were observed throughout the ingot. The largest reduction in grain size was observed at the bottom of the ingot with a gradual increase in grain size towards the top of the ingot. Stronger microstructure refinement (finer and more uniform equiaxed grain structure), as compared to inoculation, was observed when the melt was subjected to ultrasonication (without inoculation), Fig. 2c. As opposed to the chemically inoculated ingot, maximum grain refinement occurred at the top of the ingot just below the radiating face of the ultrasonic horn. Applying ultrasound to a chemically inoculated melt resulted in fine equiaxed grain structure as shown in Fig. 2d. However, a band of slightly coarser grains can be observed at the top of the ingot (Fig. 2d) corresponding to the remnant liquid that solidified following (earlier) withdrawal of the ultrasound radiator. The grain structure in this coarser band is comparable to that observed in the ingot in Fig. 2b, indicating that chemical inoculation alone was responsible for grain formation in this area. It, therefore, appears that ultrasonication played the dominant role in the grain refinement observed in the ingot undergoing both chemical and physical refinement simultaneously (Fig. 2d). Fig. 2 clearly suggests a more effective microstructural refinement under ultrasonication of the solidifying melt as compared to chemical inoculation of the melt.

Optical micrographs from the ingots shown in Fig. 2 are presented in Fig. 3 illustrating the detailed solidification grain structure formed in the respective samples. The average grain sizes along the central vertical axis from the top to the bottom of the ingot (from just below the radiating horn in case of ultrasonicated sample) are plotted as a function of distance in Fig. 4. Both figures 3 and 4 confirm the extent of grain refinement observed in the macrostructures of ingots solidified under chemical or physical refinement conditions. Without any refinement, the base microstructure consists

of well-developed coarse dendritic grains (Fig. 3a) with an average grain size ranging between 6 to 8 mm in various regions of the solidified ingot. Complete conversion to fine equiaxed grain structure is observed following chemical refiner addition (Fig. 3b) with an average grain size varying from 395 ±38 μm at the top of the ingot to 250 ±21 μm near the bottom edge of the ingot, where the finest grain structure is observed. It should be noted that despite 1% addition level the refining efficiency of Al-5Ti-1B observed in the present experiment appears to be well below the normal acceptance level in standard TP-1 tests, where an average grain size smaller than 220 μm is considered as effective refinement in inoculated Al-alloys [1]. In order to ensure reproducibility of the observed results, chemical grain refinement experiments were repeated several times with two different batches of the master alloy, all resulting in similar grain size distribution in the solidified ingots. It is thought that the slower cooling rate in the present experiments, as compared to the cooling conditions for standard TP-1 grain refinement test, resulted in the larger than anticipated grain size. There could also be prominent recalescence at such slow cooling, reducing the effectiveness of the chemical refiner.

The ingots solidified under ultrasonication revealed very effective microstructural refinement with uniform and equiaxed grain structure forming throughout the ingot. The measured average grain size varied between 168 ±19 μm at the top (near the ultrasonic horn) to 271 ±44 μm at the bottom edge of the ingot. The extent of grain refinement is far superior to the observed chemical refinement in most parts of the ingot, especially in the region surrounding the ultrasonic horn, as shown in Figs. 3 and 4. Only towards the edge of the ingot, chemical refinement produced grain size comparable to ultrasonic induced refinement. Using ultrasonication in conjunction with chemical inoculation consistently produced the finest grain structure in the ingots, better than the refinement achieved using either chemical refinement or ultrasonication in isolation. Throughout the ingot, the average grain size

measured is below 200 μm with the finest grains forming near the ultrasonic horn with an average size of 130 ±16 μm.

3.2 Solidification microstructure in the Al-10% Cu ingots

Microstructural examination of the Al-10% Cu alloy ingots revealed similar trends in grain refinement as observed for CP-Al. However, certain differences were noted as will be indicated below. Optical micrographs from samples solidified from 725 ^{o}C under identical cooling rates but different melt treatment are shown in Fig. 5. The measured average grain sizes in different ingots are presented in Fig. 6 as a function of distance from the top along the central vertical axis. For all experiments, the grain sizes observed in the alloy ingots are finer than those obtained in CP-Al under comparable processing conditions. Without any refining (inoculation or ultrasonication), large equiaxed dendritic grains are observed (Fig. 5a) throughout the base ingot although the grains are considerably smaller than those observed in the base CP-Al ingots. Also, the dendrites have well-defined secondary arms and the variation in grain size with distance is minimal with an average of 717 ±79 μm. Chemical grain refinement using an Al-5Ti-1B master alloy triggered a drastic transformation to fine equiaxed grain structure in the entire ingot as shown in Fig. 5b. As with the unrefined ingot, the variation in grain size with distance is minimal. Also, stronger grain refinement effect is noticed in the alloy as compared to CP-Al. The average grain size measured is around 132 ±17 μm in the entire ingot, well within the acceptance level of 220 μm for effective refinement in Al-alloys [1].

Ultrasonication during solidification, with or without chemical inoculation, leads to strong refinement in grain structure throughout the entire ingots as shown in Figs. 5 and 6. As observed with CP-Al samples, the finest grains are formed just below the horn where the acoustic energy transfer is the greatest. There is a progressive increase in the grain size with the axial distance from the horn due

to the attenuation of ultrasound through the melt. Nevertheless, Fig. 6 indicates that the average grain size in the ultrasonicated samples remained consistently lower than the chemically inoculated ingots, even in the least refined section of the ingots. Surprisingly, in contrast to the observations for CP-Al, combining chemical inoculation with ultrasonication did not result in much further refinement in the grain size of the alloy ingots over only ultrasonication (Figs. 5c and 5d). Fig. 6 clearly shows that the measured average grain size in the ultrasonicated ingots have comparable values in each section irrespective of chemical inoculation.

Table 1 summarises the average grain sizes measured in ingots solidified under different treatments for both studied alloys keeping the cooling conditions identical. The results corroborate the microstructural observation. For any specific treatment, Al-10% Cu alloy produced finer grain size compared to CP-Al. Both grain refiner addition and ultrasonication promoted considerable refinement and equiaxed non-dendritic grain structure under the natural cooling conditions of the present experiments. However, the results clearly demonstrate superior physical grain refinement under ultrasonication compared to the widely-practiced conventional chemical inoculation for Al-alloys. While the addition of chemical refiner further improved the refining efficiency of ultrasonication for CP-Al, in the Al-10% Cu alloy this did not promote noticeable change in the average grain size (63 ±17 μm vs 65 ±25 μm). Table 1 also reports the average grain densities in ingots calculated assuming a space-filling geometry of spherical grains. The results are much more revealing than the grain size alone, in comparing the refinement efficiency of ultrasonication to the traditional chemical refinement. While a large increase in grain density resulted from chemical inoculation of the base CP-Al, ultrasonication alone shows a further ~100% increase in grain density over chemical grain refinement. Combining both the chemical refiner and the ultrasonication increased the grain density to almost five times over that of chemical inoculation. In the case of the Al-10% Cu alloy, ultrasonication clearly

shows much higher refining efficiency with an eight times increase in grain density over chemical inoculation. There is a small further increase in the grain density by combining chemical grain refiner with ultrasonication. The calculated average shape factor of the grains is also reported in Table 1, with a value of 1 indicating a perfectly spherical particle. A higher value of the shape factor after ultrasonication compared to the grains after chemical refinement supports a more equiaxed shape of the grains formed under ultrasonication.

3.3 Origin of grain refinement in the ultrasonicated ingots

The average ultrasound energy transmission rate through a unit propagation area is expressed as [21],

$I = ½\ \rho c\ (2\pi f A)^2$

where, ρ is the density of the melt, c the propagation velocity of sound, f and A the frequency and the amplitude of ultrasound, respectively. Estimating c as 1.3×10^3 ms^{-1} [15] and ρ_{AL} as 2.385 g/cm^3 [27], energy transmission in the present experiment can be calculated as 1500 Wcm^{-2} for an amplitude of 25 μm. This is well above the reported cavitation threshold of 100 Wcm^{-2} in Al melt [15]. Moreover, inclusions in commercial purity melt are stated to reduce the cavitation threshold further [23]. Developed cavitation is thus expected in the ultrasonicated melts and semi-liquid slurry and likely responsible for the observed physical refinement of microstructure.

It should be noted that soluble Ti has a strong growth restriction effect in Al-melt. There is a possibility of Ti dissolution from the horn contributing to the observed grain refinement in the ultrasonicated Al-melt. Compositions determined through optical emissions spectroscopy of Al-10% Cu alloy ingots processed under different conditions are presented in Table 2. Ti concentration varied between different ultrasonicated ingots and the observed range of concentration is given for various

regions in the ingots. Although no visible degradation of the horn was observed, Ti pickup in the melt under ultrasonication is noted especially close to the horn. This would contribute growth restriction of solid particles near the horn. However, the growth restriction and constitutional undercooling alone does not fully explain the high grain density in the absence of potent nucleants under ultrasonication. Most importantly, a higher level of soluble Ti, along with highly potent nucleant particles, is present in the chemically inoculated ingot. Yet the extent of chemical grain refinement is inferior to the physical refinement in ultrasonicated ingots. Therefore, the observed grain refinement is thought to be contributed by other factors rather than soluble Ti under ultrasonication.

The cooling rates measured from the linear sections of the cooling curves under different treatment conditions are presented in Table 1 for the Al-10% Cu alloy. Ultrasonication increases the overall cooling rate but not drastically to account for the observed grain refinement compared to the base alloy. However, significant slowing down of the cooling rates for the cases of chemical inoculation and ultrasonication is observed just before recalescence with cooling rates of 41, 36, 32 and 34 K min^{-1} for the base alloy, chemical inoculation, ultrasonication and combined refinement, respectively. This may indicate increased nucleation activity under chemical inoculation and ultrasonication. Figure 7 compares enlarged sections of the cooling curves relevant to α-Al solidification in the Al-10% Cu ingot samples under different treatment conditions. Increased noise seen in the curves for the ultrasonicated samples is due to the proximity of the thermocouple to the horn, but the general trends of solidification can be observed. As expected, base alloy shows largest melt undercooling with a minimum temperature recorded at 618.5 ^{o}C. On chemical inoculation, there is a prominent decrease in the maximum undercooling with a minimum recorded melt temperature of 623 ^{o}C. Ultrasonication indicates a maximum melt undercooling comparable to chemical inoculation with a recorded minimum also at 623 ^{o}C. That chemical refiner addition did not contribute to further

refinement under ultrasonication is also substantiated by the identical nature of the cooling curves recorded in both cases of sonication. This suggests that heterogeneous nucleation under ultrasonication could be as effective as inoculation through Al-5Ti-1B chemical refiner.

4. Discussion

Two key mechanisms are generally attributed to grain refinement under ultrasonication. As the ultrasonication was performed during solidification, one obvious reason for the observed grain refinement is mechanical fragmentation of growing dendrites in the region of cavitation. Cavitation induced fragmentation of well-developed dendrites have directly been observed in non-metallic analogue system [28]. For metallic systems solidifying under melt flow, dendrite fragmentation may also occur through local rise in temperature or solute concentration affected by the convective fluid flow [29]. Fragmented dendrite arms are then distributed in the bulk melt through acoustic streaming and contribute to grain multiplication through survival. Table 1 reports the measured average secondary dendrite arm spacing (SDAS) of 372 μm for CP-Al and 86 μm for Al-10%Cu alloy base ingots. Under comparable cooling environment, the measured average grain sizes of 233 μm and 65 μm in the ultrasonicated CP-Al and Al-10%Cu ingots are finer than the respective SDAS. The smaller grain size compared to the SDAS, and the lack of any remnant primary dendrite stem in the entire ultrasonicated ingot microstructure would require substantial fragmentation during very early stages of dendrite evolution and the number of fragments being significant enough to produce a fine equiaxed grain structure. The extent of cavitation induced fragmentation of very small mobile dendrites at the early stages of their growth needs to be further investigated in metallic systems.

Enhanced heterogeneous nucleation under ultrasonication can be attributed to forced wetting of the endogenous substrates such as the mould wall and non-metallic inclusions. However, these

inefficient nucleants would require larger nucleation undercooling than potent nucleants in the Al-5Ti-1B inoculated Al-melt where heterogeneous nucleation is triggered at undercooling as low as 0.2 ^{o}C [30]. Previous investigation reported no grain refinement when superheated melt was ultrasonicated prior to nucleation [31] suggesting limited influence of forced wettings of inclusions on nucleation enhancement under sonication. The nucleation initiation temperature can be effectively estimated from the first derivative of temperature with time (deflection in the slope) in the cooling curves. Analysis of the derivative of cooling curves indicate nucleation initiation temperatures of 620, 625, 624 and 625 ^{o}C for the solidification of base, chemically inoculated, and ultrasonicated melts without and with refiner addition, respectively. The slightly higher nucleation temperature for Al-5Ti-1B refined alloy, as compared to purely ultrasonicated ingots, probably indicates higher nucleation potency under chemical inoculation. Nevertheless, the observed increase in the nucleation temperature (and the associated high nucleation potency) under ultrasonication is difficult to explain purely on the basis of forced wetting of natural substrates under cavitation. An alternative mechanism of pressure induced shift of the melting point has been proposed [25] and used as a plausible explanation for enhanced nucleation under cavitation in metallic melts [15, 32]. This shift in melting point provides additional undercooling to activate already wetted natural substrates enhancing heterogeneous nucleation in ultrasonicated melts. Recent in-situ small angle X-ray scattering (SAXS) investigation indicated cavitation enhanced nucleation under ultrasonication in an Al-15wt.% Cu alloy melt above its liquidus temperature [33].

The large increase in grain number density in the ultrasonicated ingots compared to chemically inoculated ingots, as reported in Table 1, needs to be examined. It appears that although the potency of heterogeneous nucleants is higher in the Al-5Ti-1B inoculated melt, more nucleation events have occurred in the ultrasonicated melt. Similar results have been reported for Mg-alloys, where smaller

grains and larger grain density were observed under ultrasonication as compared to the base alloy or chemical inoculation [15]. For inoculated Al- and Mg- alloys, only a small fraction of the potent nucleants is reported to contribute to grain formation [2, 15]. While efficient refiners initiate nucleation at extremely low undercooling, only the largest size particles act as transformation nuclei leading to free growth [2]. Following the release of latent heat (recalescence), majority of the smaller particles do not contribute to grain formation. An estimate for Al shows the minimum size of TiB_2 particle actively contributing to grain formation to be 3 μm [2]. Figure 7 clearly shows distinct recalescence following nucleation in the base and chemically inoculated ingots in the present experiment. In contrast, ultrasonicated ingots do not indicate any prominent recalescence in Fig. 7. Effective dissipation of the latent heat under the intense convection created through ultrasonication may prolong nucleation and larger fraction of the available nucleants can contribute to grain formation as compared to chemical inoculation, even though the latter may have higher nucleation potency. This also explains the previous observation of increased number of Zr particles contributing to nucleation under ultrasonication in a Zr-inoculated Mg-melt [15] and the increased effectiveness of inoculation under ultrasonication in the CP-Al ingots in the present study.

Another important observation from the present experiments is the large reduction in grain size (or increase in grain density) under ultrasonication in the Al-10% Cu alloy as compared to CP-Al. This is normally expected due to the growth restriction and constitutional undercooling effect of solute under quiet solidification condition. Also, chemical inoculation of the Al-10% Cu alloy did not substantially improve the refinement effect of ultrasonication, indicating high nucleation efficiency under ultrasonication alone. The general perception is that strong fluid flow generated under cavitation may homogenise the solute distribution at the solid-liquid interface reducing the constitutional

undercooling effect. However, presence of solute appears to further enhance the grain refining effect of ultrasound and this effect needs further investigation.

It should be noted that while the indirect evidence from the present experiment suggests enhanced nucleation being a major contributor to grain refinement under ultrasonication, it is probable that both dendrite fragmentation and enhanced nucleation are active. The dominance of one mechanism over the other likely depends on the solidification conditions. Further studies in metallic systems, in particular direct observation of grain formation under cavitation, would be necessary to understand and clarify the exact mechanism of microstructure formation under ultrasonication.

5. Conclusions

Microstructural refinement under ultrasonication is examined under natural air cooling of commercial purity Al (CP-Al) as well as binary Al-10 wt% Cu alloy melts. The effectiveness of refinement is compared against chemical inoculation using the standard Al-5Ti-1B master alloy under identical cooling conditions.

Both chemical inoculation and ultrasonication produced fine equiaxed grain structure, eliminating the coarse dendritic microstructure observed in the unrefined base ingots. Grain size in the chemically refined ingots was finest near the mould wall (bottom and sides of the ingot) and increased towards the top free surface. In contrast, ultrasonicated ingots showed the finest grain size at the top (just below the radiator) and a progressively increasing grain size toward the mould wall.

For the CP-Al ingots, ultrasonication produced finer grains in most areas of the ingot compared to chemical inoculation. Combining ultrasonication with chemical inoculation resulted in the finest observed grain size distribution in the entire ingot. In the Al-10 wt% Cu ingots, the efficiency of ultrasound-induced grain refinement was drastically superior to chemical grain refinement with almost

8 times increase in the grain density. Combining with chemical inoculation did not further improve the refining efficiency of ultrasonication to any appreciable extent.

The cooling curves measured under ultrasonication and chemical inoculation show identical reduction in the maximum nucleation undercooling compared to the unrefined base ingots. However, distinct recalescence observed following nucleation in the chemically inoculated melt was largely eliminated in the ultrasonicated melts.

Indirect evidence appears to suggest a major contribution from enhanced heterogeneous nucleation on the observed grain refinement under ultrasonication in the present experiments though some contribution from fragmentation cannot be ruled out.

The superior refinement observed under ultrasonication over chemical inoculation seems to be contributed by larger number of grain initiation from efficient dissipation of latent heat under strong convection despite chemical refiners having better nucleating potency.

References

[1] B.S. Murty, S.A. Kori, M. Chakraborty, Int. Mater. Rev. 47 (2002) 3-29.

[2] A.L. Greer, P.S. Cooper, M.W. Meredith, W. Schneider, P. Schumacher, J.A. Spittle, A. Tronche, Adv. Eng. Mater. 5 (2003) 81-91.

[3] D.H. StJohn, M. Qian, M.A. Easton, P. Cao and Z. Hildebrand, Metall. Mater. Trans. A, 36 (2005) 1669-1679.

[4] J.A. Spittle, Int. Mater. Rev. 51 (2006) 247-269.

[5] M.A. Easton, M. Qian, A. Prasad, D.H. StJohn, Current Opinion in Solid State and Materials Science 20 (2016) 13–24

[6] D. Qiu, J.A. Taylor, M-X. Zhang and P.M. Kelly, Acta Mater. 55 (2007) 1447–1456.

[7] C. Limmaneevichitr and W. Eidhed, Mater. Sci. Eng. A349 (2003) 197–206.

[8] A. M. Bunn, P. Schumacher, M. A. Kearns, C. B. Boothroyd and A. L. Greer, Mater. Sci. Tech. 15 (1999) 1115-1123.

[9] A.M. Detomi, A.J. Messias, S. Majer and P.S. Cooper, in: Light Metals, J.L. Anjier (Ed.), TMS, New Orleans, LA, 2001, pp.919-925.

[10] A. Das, G. Liu, Z. Fan, Mater. Sci. Eng. A419 (2006) 349-356.

[11] M. Li, T. Tamura and K. Miwa, Acta Mater. 55 (2007) 4635-4643.

[12] D. Räbiger, Y. Zhang, V. Galindo, S. Franke, B. Willers and S. Eckert, Acta Mater. 79 (2014) 327-338.

[13] K.Kocatepe and C.F. Burdett, J Mater. Sci. 35 (2000) 3327-3335.

[14] G.I. Eskin, Ultrasonic Treatment of Light Alloy Melts, Gordon and Breach, 1998.

[15] A. Ramirez, Ma Qian, B. Davies, T. Wilks, D.H. StJohn, Scripta Mater. 59 (2008) 19-22.

[16] Ma Qian, A. Ramirez, A. Das, J. Cryst. Growth, 311 (2009) 3708-3715.

[17] V. Abramov, O. Abramov, V. Bulgakov, F. Sommer, Mater. Lett. 37 (1998) 27-34.

[18] G.I. Eskin, Ultrasonic Sonochemistry 8 (2001) 319-325.

[19] X. Xian, T.T. Meek, Q. Han, Scripta Mater. 54 (2006) 893-896.

[20] C. Ruirun, Z. Deshuang, G. Jingjie, M. Tengfei, D. Hongsheng, S. Yanqing and F. Hengzhi, Mater. Sci. Eng. A 653 (2016) 23-26.

[21] S.V. Komarov, M. Kuwabara, O.V. Abramov, ISIJ International 45 (2005) 1765-1782.

[22] Li Xin-tao, Li Ting-ju, Li Xi-meng, Jin Jun-ze, Ultrasonic Sonochemistry 13 (2006) 121-125.

[23] G.I. Eskin, D.G. Eskin, Ultrasonic Sonochemistry 10 (2003) 297-301.

[24] Y. Tsunekawa, H. Suzuki, Y. Genma, Materials and Design 22 (2001) 467-472.

[25] B. Chalmers, Principles of Solidification, John Wiley & Sons, NY, 1964, pp. 86-89.

[26] J.D. Hunt, K.A. Jackson, J. Appl. Phys. 37 (1966) 254-257.

[27] E.A. Brandes, G.B. Brooke (Eds.), Smithells Metals Reference Book, Butterworth-Heinemann, OX, 1992.

[28] D. Shu, B. Sun, J. Mi and P.S. Grant, Metall. Mater. Trans. A 43A (2012) 3755-3766.

[29] A. Hellawell, S. Liu and S.Z. Lu, JOM 49 (1997) 18-20.

[30] A.L. Greer, Phil. Trans. R. Soc. Lond. A 361 (2003) 479-495.

[31] G. Wang, M.S. Dargusch, M. Qian, D.G. Eskin and D.H. StJohn, J Cryst. Growth 408 (2014) 119-124.

[32] A. Das and H.R. Kotadia, Mater. Chem. Phys. 125 (2011) 853-859.

[33] H. Huang, D. Shu, J. Zeng, F. Bian, Y. Fu, J. Wang and B. Sun, Scripta Mater. 106 (2015) 21-25.

Table 1. Average grain size data measured from the CP-Al and the Al-10%Cu ingots solidified under different condition. Microstructure throughout the ingot is used for the size measurement. SDAS represents the secondary dendrite arm spacing.

Refining method	Commercial purity Al			Al-10wt.%Cu Alloy				
	Grain size (μm)	SDAS (μm)	Grain density (mm^{-3})	Cooling rate ($^oCmin^{-1}$)	Grain size (μm)	SDAS (μm)	Shape factor	Grain density (mm^{-3})
Base alloy	6730 ± 627	372	<<1	42	717 ± 79	86	羊	5
Al-5Ti-1B (GR)	287 ± 48	羊	81	42	132 ± 17	羊	0.7	836
Ultrasonic (UT)	233 ± 37	羊	150	50	65 ± 25	羊	0.8	7052
GR + UT	169 ± 34	羊	395	48	63 ± 17	羊	0.8	7711

Table 2. Composition of Al-10wt.%Cu alloy ingots solidified under different conditions as determined through optical emissions spectroscopy.

Processing Condition	Elemental concentration (wt.%)				
	Al	Si	Fe	Cu	Ti
Unrefined	balance	0.04	0.147	9.8	0.003
Grain refined	balance	0.04	0.147	9.9	0.12
Ultrasonicated (near horn)	balance	0.04	0.147	9.8	0.06 - 0.09
Ultrasonicated (middle of ingot)	balance	0.04	0.147	9.8	0.03 – 0.05
Ultrasonicated (bottom of ingot)	balance	0.04	0.147	9.8	0.01 - 0.02

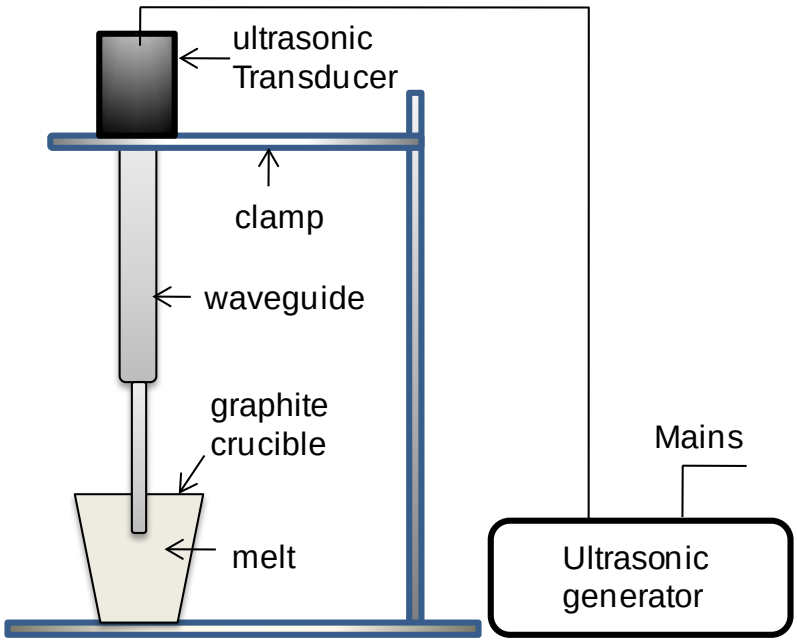

Fig. 1. Schematic illustration of the experimental setup for direct ultrasonic treatment of solidifying melt.

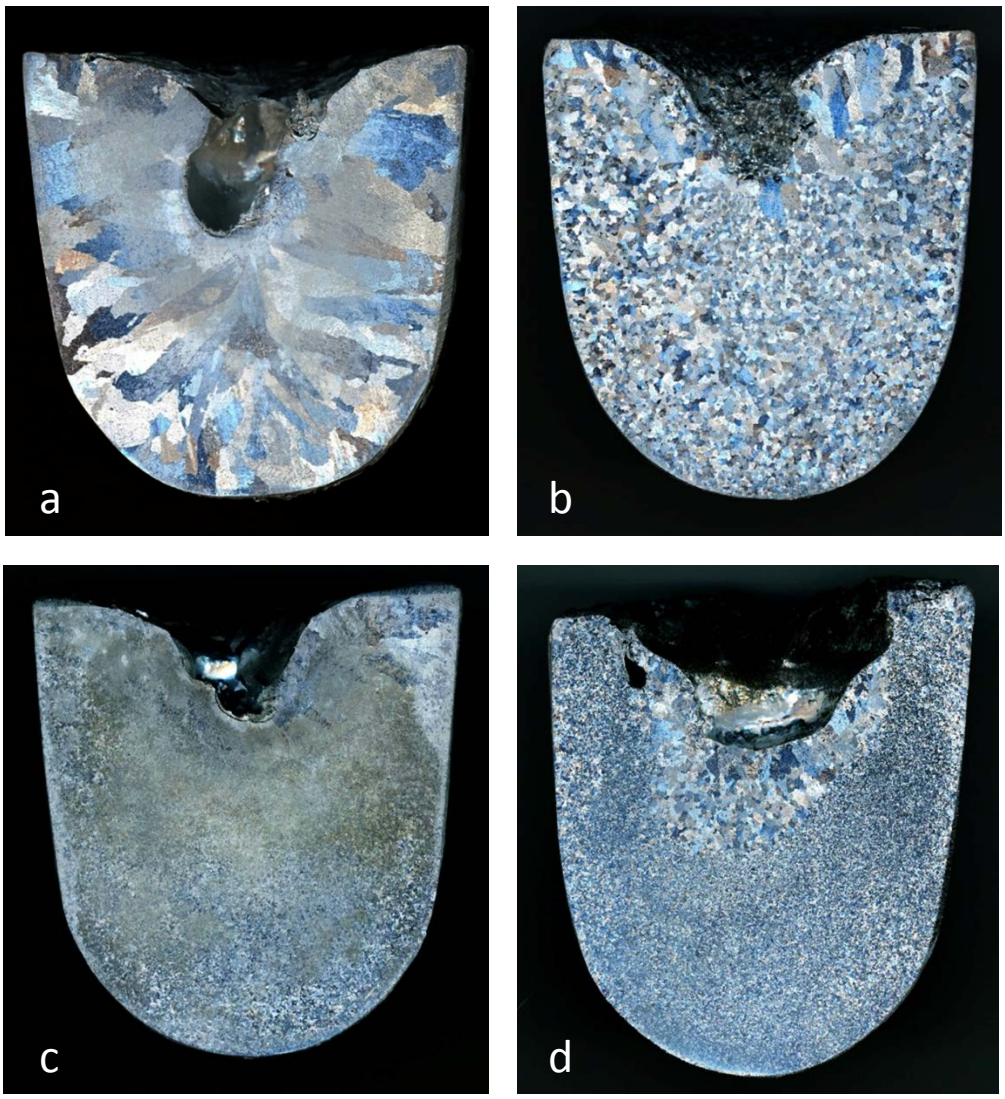

Fig. 2. Macrostructures of commercial purity Al (CP-Al) ingots solidified from 725 ^{o}C under identical slow cooling conditions subjected to (a) conventional solidification, (b) Al-5Ti-1B inoculation, (c) ultrasonication and (d) combined chemical inoculation and ultrasonication.

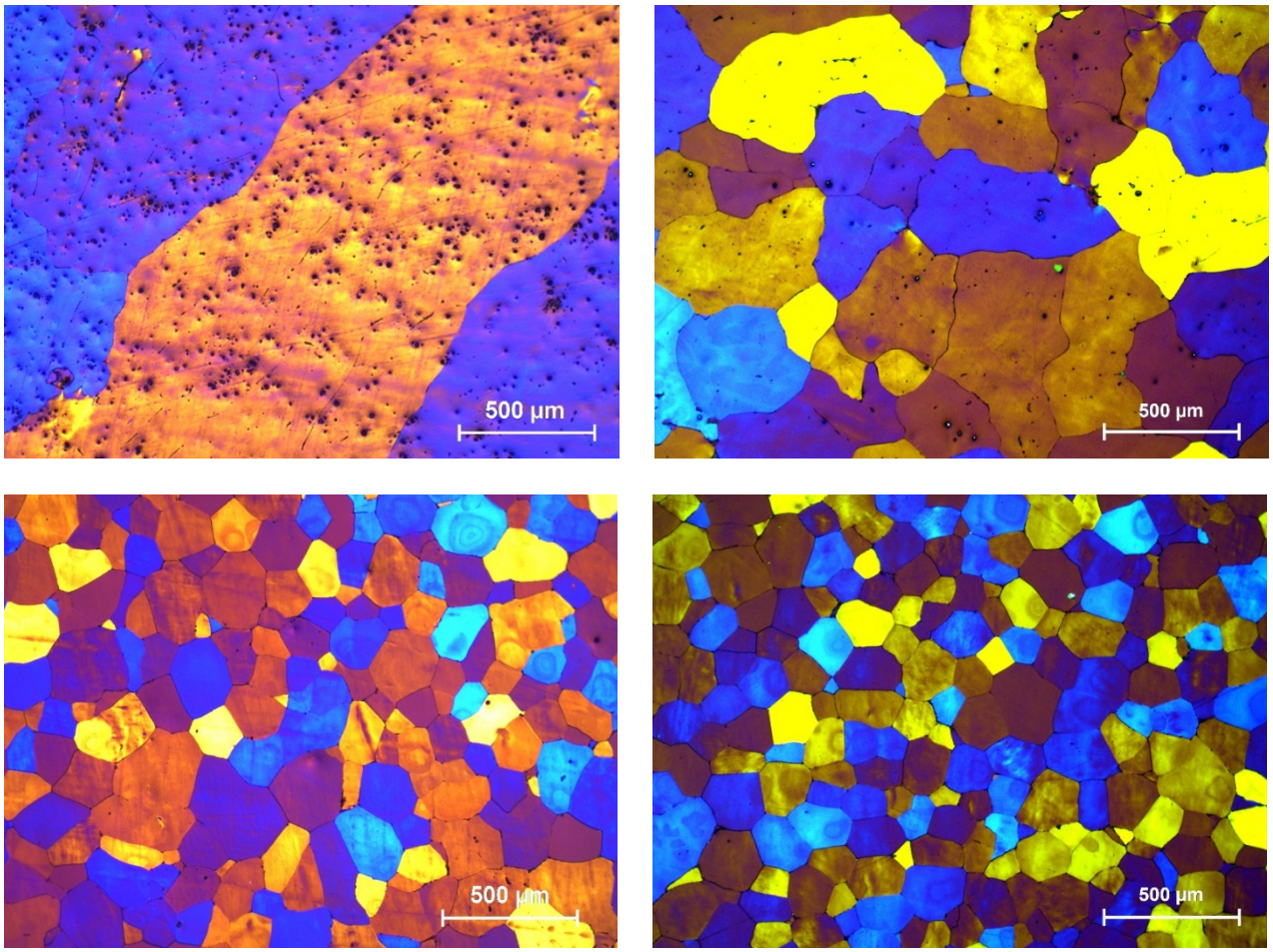

Fig. 3. Optical micrographs of CP-Al cast from 725 ^{o}C under identical cooling conditions subjected to (a) conventional solidification (b) Al-5Ti-1B inoculation (c) ultrasonication and (d) combined chemical inoculation and ultrasonication. Microstructures are presented from near the top of the ingots.

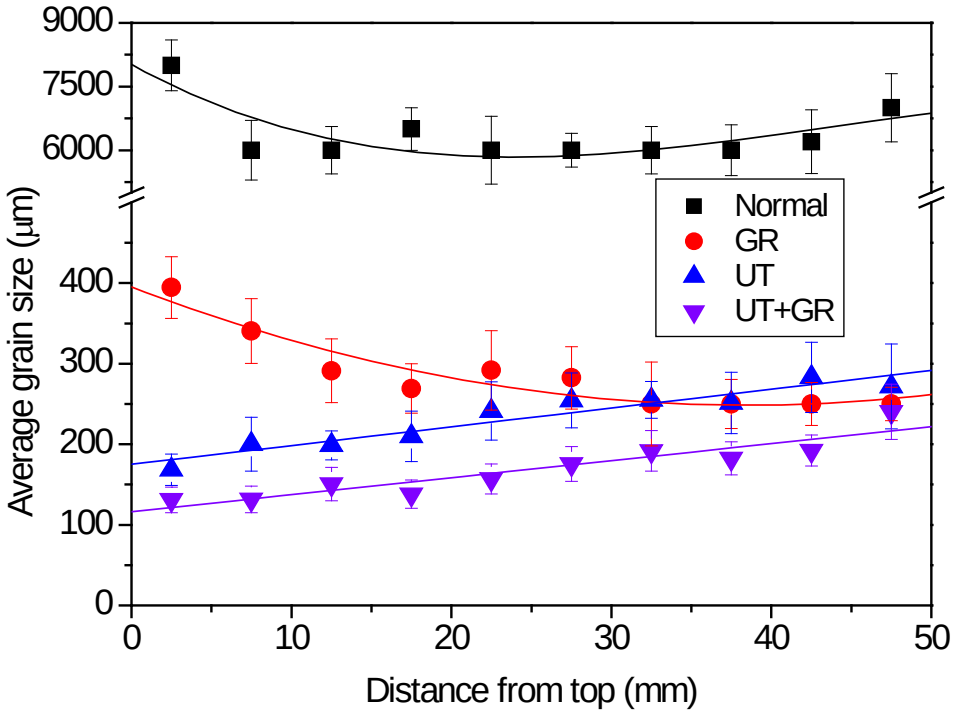

Fig. 4. Measured average grain size for CP-Al ingots as a function of distance from the top along the central vertical axis. For ultrasonicated samples, distance is measured from the tip of the radiator.

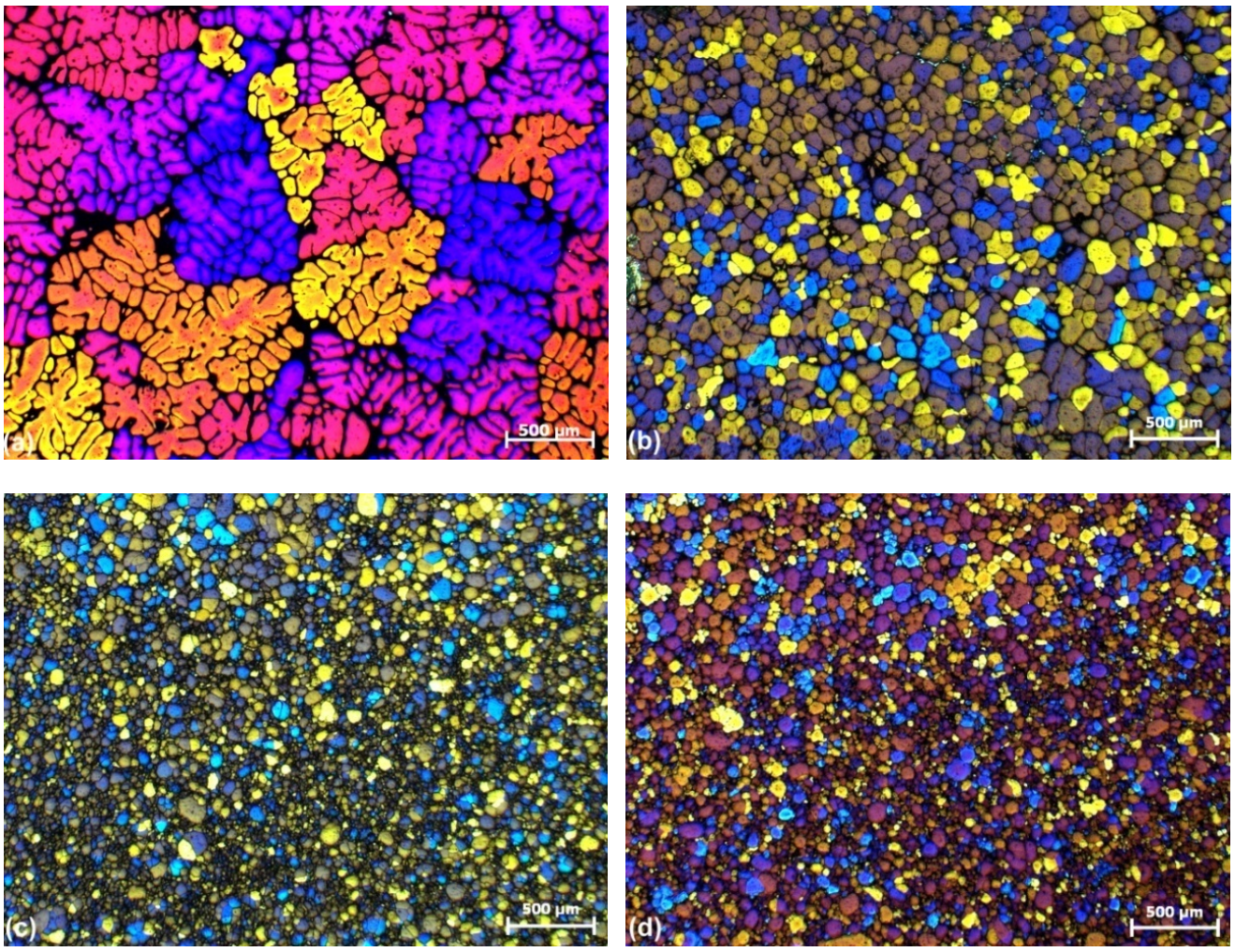

Fig 5. Optical micrographs from Al-10%Cu alloy ingots cast under various conditions: (a) conventionally cast (b) Al-5Ti-1B inoculated (c) Ultrasonicated (d) Inoculated and ultrasonicated. All samples were cast at 725 °C.

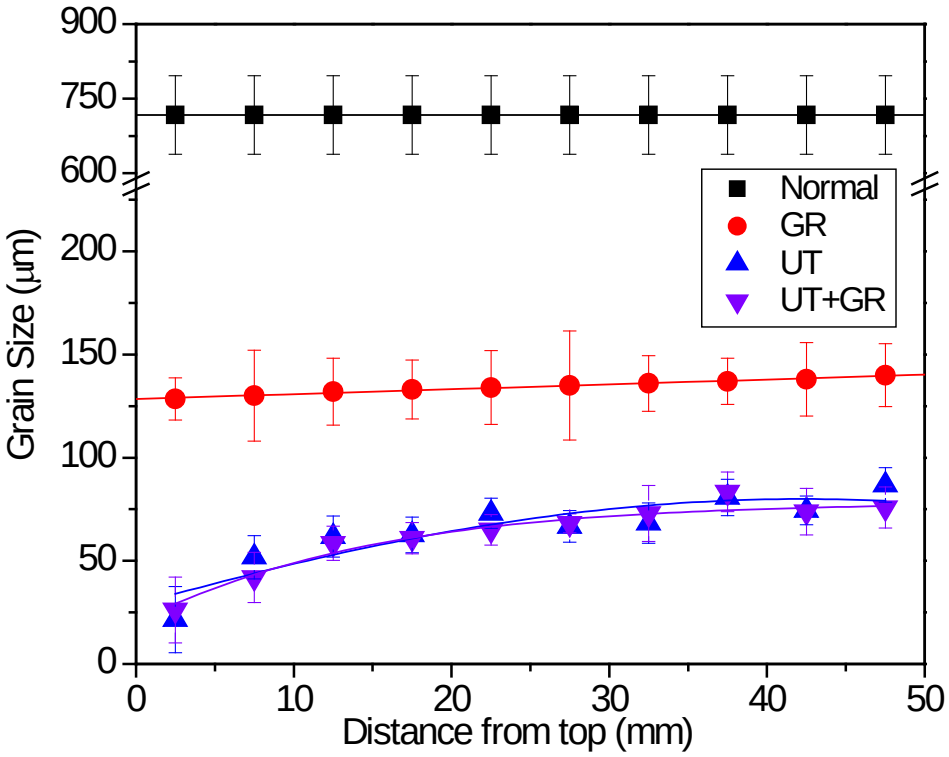

Fig. 6. Measured average grain size for Al-10%Cu alloy ingots as a function of distance from the top along the central vertical axis. For ultrasonicated samples distance is measured from the tip of the radiator.

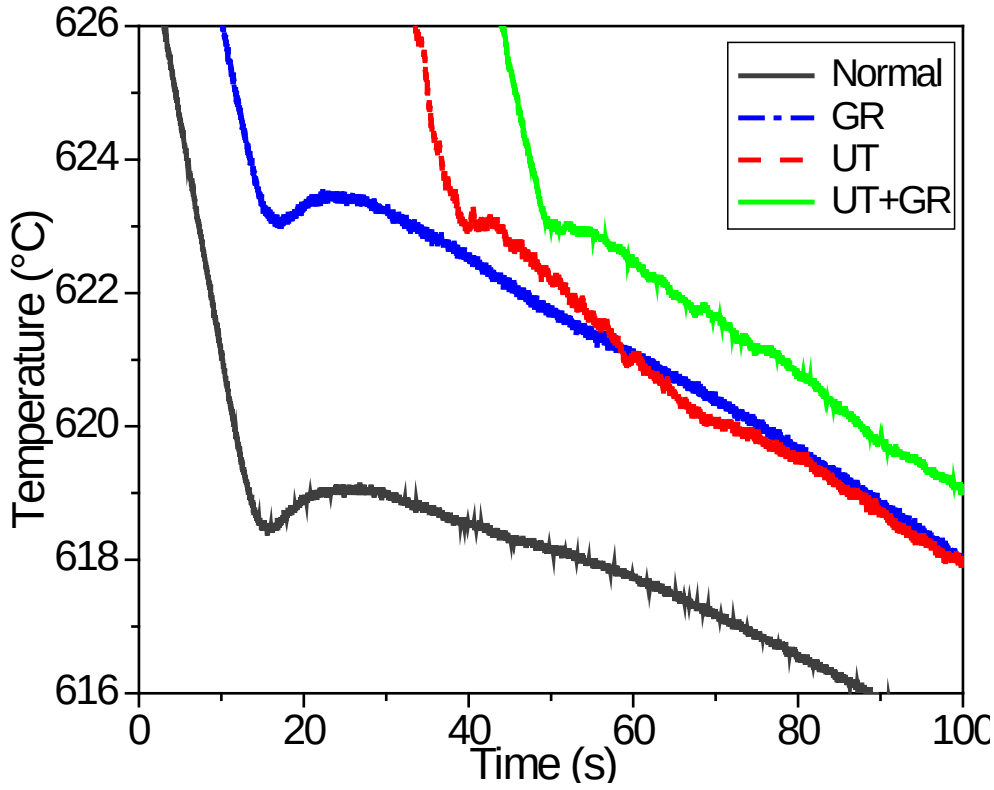

Fig. 7. Enlarged sections of the measured cooling curves from Al-10wt.% Cu ingots solidified under different conditions illustrating formation of α-Al grains. GR, UT and UT+GR represent chemical inoculation, ultrasonication and combined ultrasonic and chemical inoculation, respectively.